Supporting Information

Covalent Functionalization of Tin Disulfide with Porphyrin for Ultrafast Optical Limiting

Zhiyuan Wei,[†] Yan Fang,[†] Hui Li,[†] Zihao Guan,[†] Naying Shan,[†] Fang Liu,[†] Yang Zhao,[†] Lulu Fu,*,[†] Zhipeng Huang,[†] Mark G. Humphrey,*,[‡] Chi Zhang*,[†]

[†] *School of Chemical Science and Engineering, Tongji University, Shanghai, 200092, China*
[‡] *Research School of Chemistry, Australian National University, Canberra, ACT 2601, Australia*

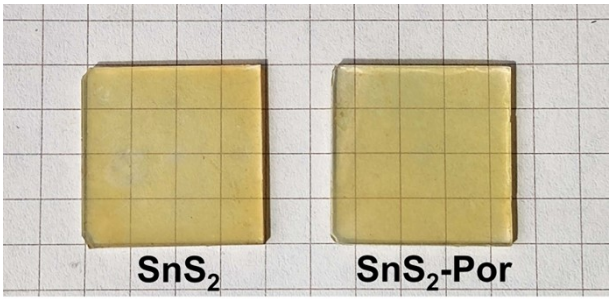

Figure S1. Photographs of the SnS_2 nanosheets and the SnS_2-Por nanohybrid.

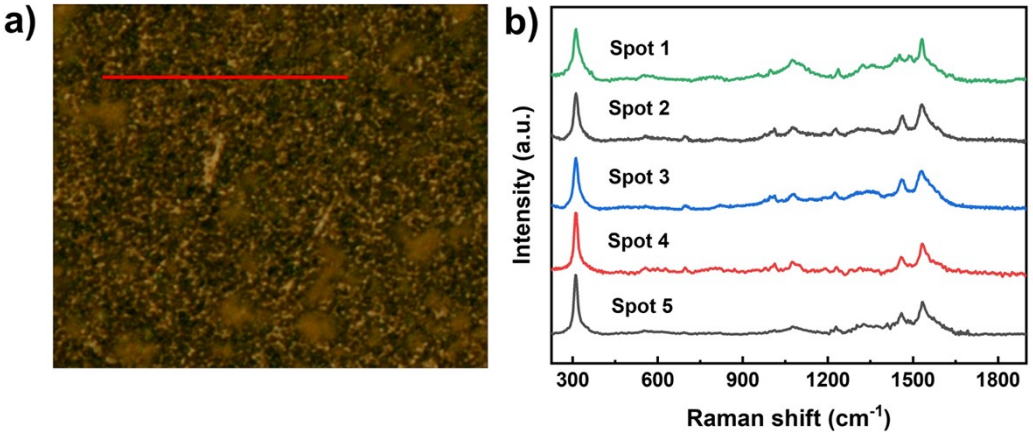

Figure S2. (a) The optical microscopy of the SnS_2-Por nanohybrid. (b) The Raman spectra of 5 spots along the red line in (a).

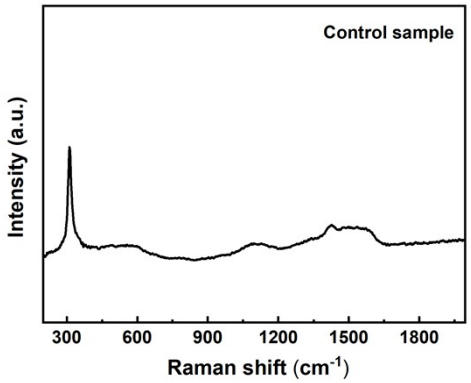

Figure S3. Raman spectrum of the control sample.

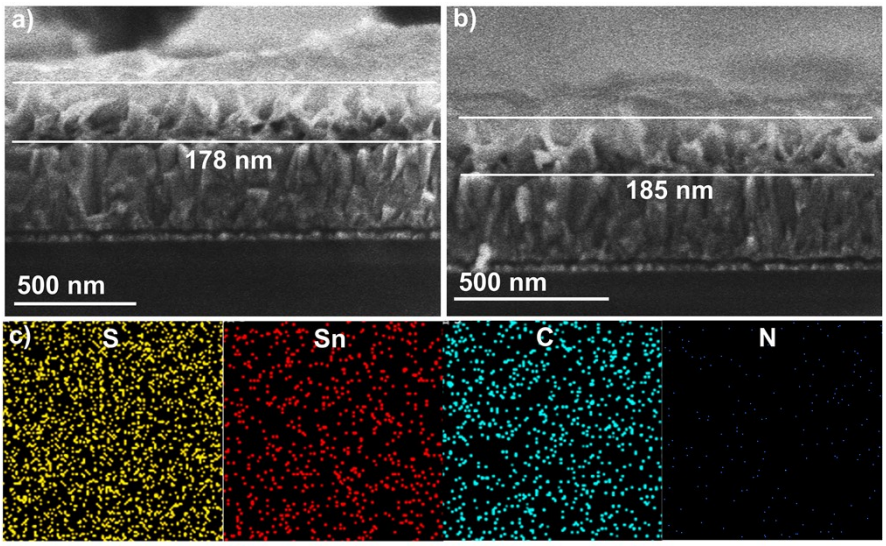

Figure S4. (a) Cross-sectional view SEM image of the SnS_2 nanosheets. (b) Cross-sectional view SEM image of the SnS_2-Por nanohybrid. (c) Elemental mapping images of the SnS_2 nanosheets.

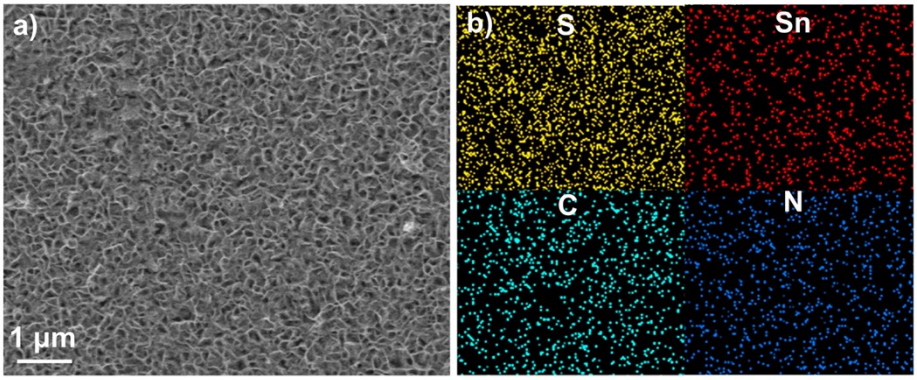

Figure S5. SEM image (a) and the corresponding elemental mapping images (b) of the SnS_2-Por nanohybrid on a larger scale.

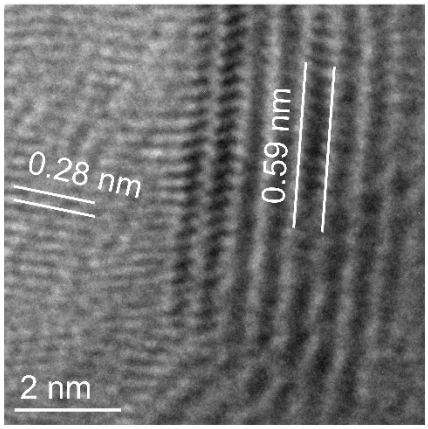

Figure S6. High-resolution TEM image of the SnS_2-Por nanohybrid.

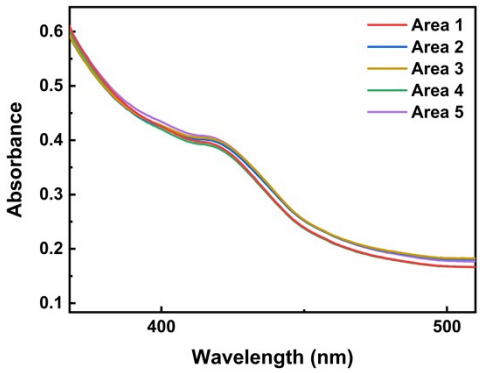

Figure S7. UV-Vis absorption spectra of the SnS_2-Por nanohybrid at different areas.

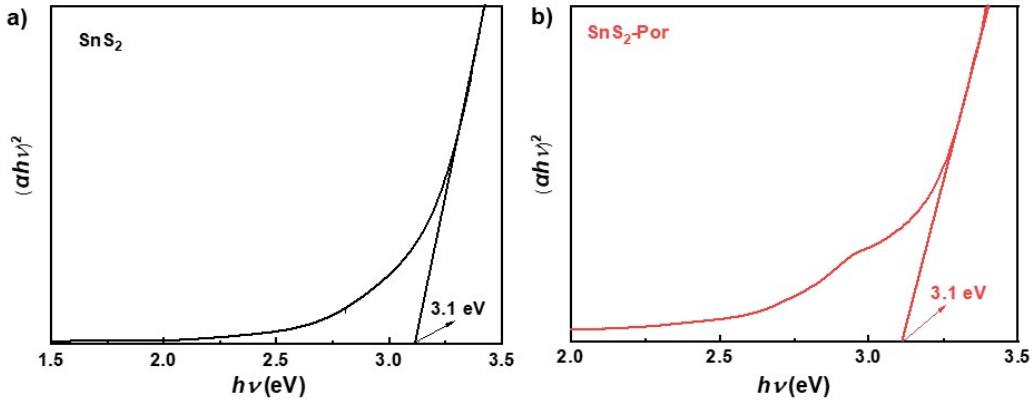

Figure S8. Tauc plots of the SnS_2 nanosheets (a) and the SnS_2-Por nanohybrid (b).

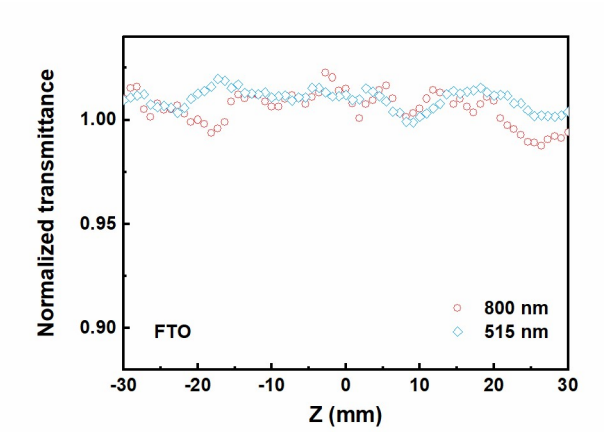

Figure S9. Open-aperture Z-scan curves of the FTO substrate at 800 nm with 56 nJ pulse energy and at 515 nm with 60 nJ pulse energy.

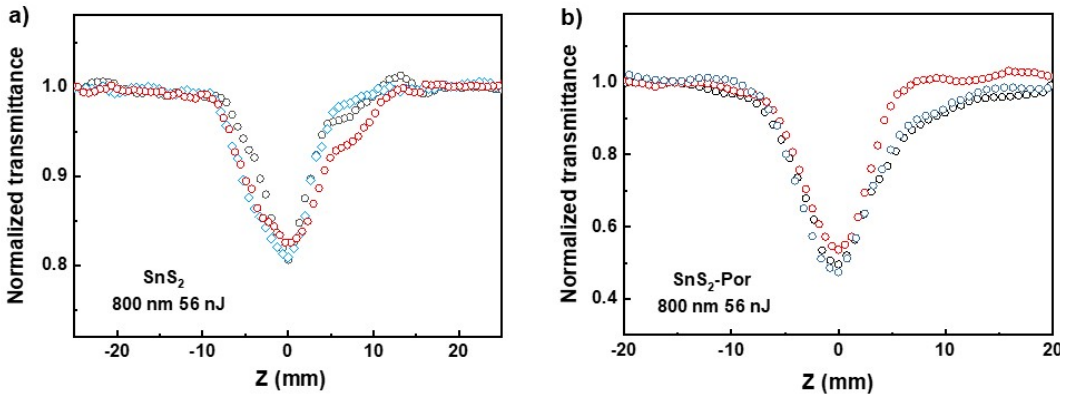

Figure S10. Open-aperture Z-scan curves measured at different points of the SnS_2 nanosheets (a) and the SnS_2-Por nanohybrid (b).

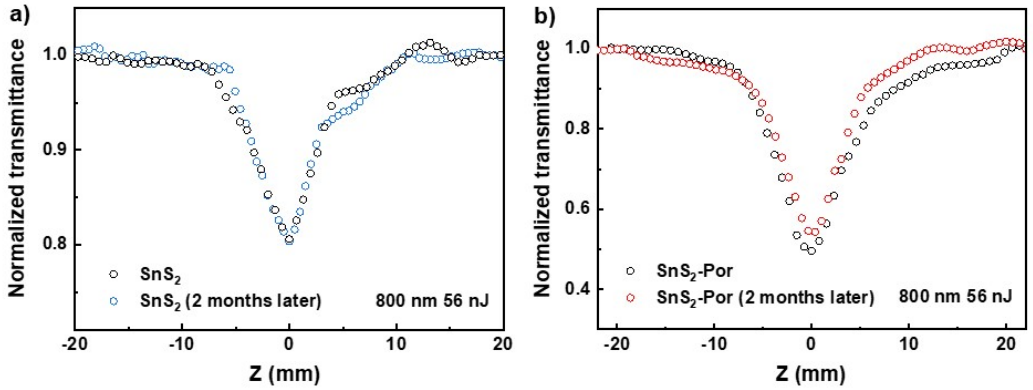

Figure S11. Open-aperture Z-scan curves of the SnS_2 nanosheets (a) and the SnS_2-Por nanohybrid (b) before and after ambient exposure.

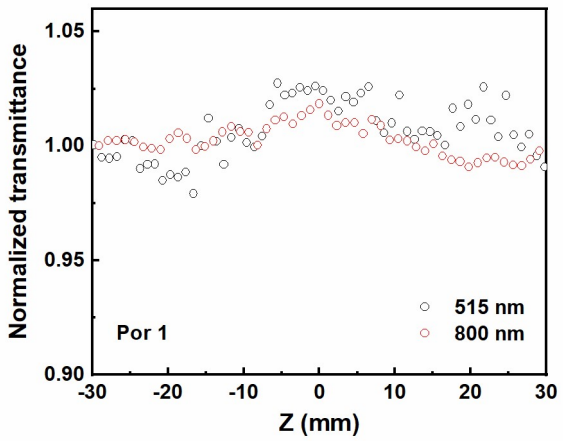

Figure S12. Open-aperture Z-scan curves of Por **1** solutions at 800 nm with 56 nJ pulse energy and at 515 nm with 60 nJ pulse energy.

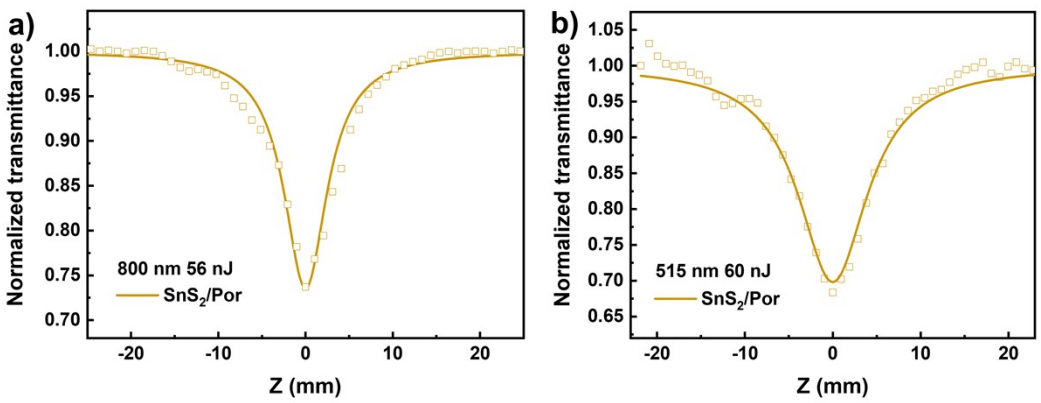

Figure S13. Z-scan curves of the SnS_2/Por blend at 800 nm (a) and 515 nm (b).

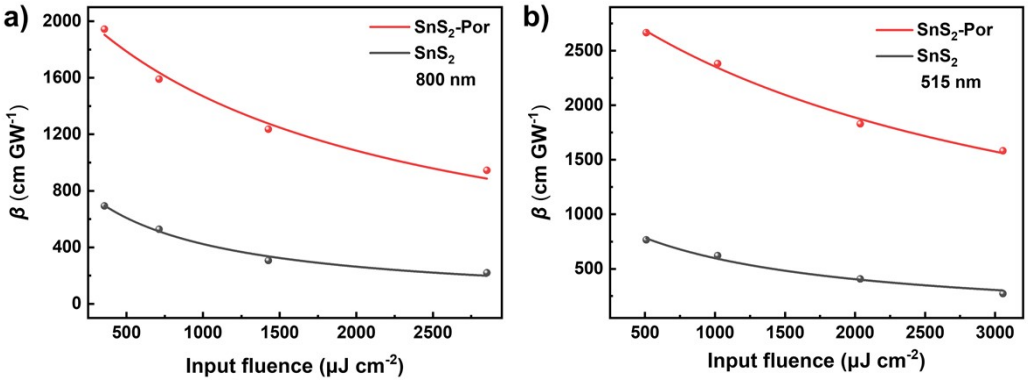

Figure S14. TPA saturation fitting at 800 nm (a) and 515 nm (b).

Table S1. Atom percentages of the SnS_2 nanosheets and the SnS_2-Por nanohybrid.

Element	Atom (%)	
	SnS_2	SnS_2-Por
Sn 3d	14.21	11.70
S 2p	25.55	20.76
C 1s	37.81	43.53
O 1s	22.44	16.47
N 1s	-	7.54

Table S2. Optical limiting thresholds (F_{th}) at selected wavelengths.

Materials	Laser	F_{th} (mJ cm^{-2})
SnS_2-Por (this work)	515 nm 35 fs 1 kHz	1.65
Azine derivative[1]	515 nm 190 fs 20 Hz	16
hydrazone derivative[2]	515 nm 190 fs 20 Hz	2.75
SWNTs[3]	532 nm 5 ns	250
SWNT-TPP[3]	532 nm 5 ns	70
Graphene[4]	532 nm 6 ns 10 Hz	800
Graphene-Zn-porphyrin[4]	532 nm 6 ns 10 Hz	200
ZnTPyP-1/PDMS[5]	532 nm 5 ns 5 Hz	320
WS_2[6]	532 nm 7 ns 10 Hz	880
GO:PVA[7]	400 nm 100 fs 1 kHz	1.6
SnS_2-Por (this work)	800 nm 35 fs 1 kHz	2.74
MoS_2/PMMA[8]	800 nm 100 fs 1 Hz	35.2
WSe_2[9]	800 nm 130 fs 1 kHz	21.6
Pc-pyrene PMMA film[10]	800 nm 90 fs 1 kHz	1.8
Carbon nanodots[11]	800 nm 100 fs 1 kHz	74
GO films[12]	800 nm 100 fs 1 kHz	37
Al-doped InSe thin film[13]	800 nm 190 fs 10 Hz	14
$Li_{0.952}Sn^{II}_{0.398}Sn^{IV}_{0.563}S_2$[14]	800 nm 35 fs 1 kHz	0.8

Table S3. Linear optical and NLO parameters of the SnS_2/Por blend.

Samples	Laser	α_0 (cm^{-1})	T (%)	β_{eff} (cm GW^{-1})
SnS_2/Por	800 nm 56 nJ	18833	70	323 ± 10
	515 nm 60 nJ	30828	55	409 ± 10

Table S4. NLO parameters of the SnS_2 nanosheets and the SnS_2-Por nanohybrid

Laser	Samples	β_0 (cm GW^{-1})	I_s (μJ cm^{-2})
800 nm 35 fs	SnS_2	1083 ± 111	641 ± 135
	SnS_2-Por	2280 ± 117	1815 ± 287
515 nm 35 fs	SnS_2	1140 ± 103	1101 ± 215
	SnS_2-Por	3129 ± 76	3041 ± 246

Reference

1. Z. Xiao, J. Ge, R. Sun, Y. Fang, Y. She, Z. Li, X. Wu, S. Liu, L. Li, Y. Jian and Y. Song, *Opt. Mater.*, 2018, **83**, 300-305.
2. J. Jia, X. Wu, Y. Fang, J. Yang, X. Guo, Q. Xu, Y. Han and Y. Song, *J. Phys. Chem. C*, 2018, **122**, 16234-16241.
3. Z. B. Liu, J. G. Tian, Z. Guo, D. M. Ren, T. Du, J. Y. Zheng and Y. S. Chen, *Adv. Mater.*, 2008, **20**, 511-515.
4. M. B. M. Krishna, V. P. Kumar, N. Venkatramaiah, R. Venkatesan and D. N. Rao, *Appl. Phys. Lett.*, 2011, **98**, 081106.
5. D. J. Li, Q. H. Li, Z. R. Wang, Z. Z. Ma, Z. G. Gu and J. Zhang, *J. Am. Chem. Soc.*, 2021, **143**, 17162-17169.
6. T. Abhijith, S. E, R. Suthar, P. Sharma, S. Thomas, S. Karak, *Nanotechnology*, 2022, **33**, 435702.
7. X.-F. Jiang, L. Polavarapu, H. Zhu, R. Ma and Q.-H. Xu, *Photonics Res.*, 2015, **3**, A87-A91.
8. G. Liang, L. Tao, Y. H. Tsang, L. Zeng, X. Liu, J. Li, J. Qu and Q. Wen, *J. Mater. Chem. C*, 2019, **7**, 495-502.
9. X. Tian, R. Wei, Q. Guo, Y. J. Zhao and J. Qiu, *Adv. Mater.*, 2018, **30**, 1801638.
10. A. Husain, A. Ganesan, M. Sebastian and S. Makhseed, *Dyes Pigm.*, 2021, **184**, 108787.
11. D. Tan, Y. Yamada, S. Zhou, Y. Shimotsuma, K. Miura and J. Qiu, *Carbon*, 2014, **69**, 638-640.
12. X. F. Jiang, L. Polavarapu, S. T. Neo, T. Venkatesan and Q. H. Xu, *J. Phys. Chem. Lett.*, 2012, **3**, 785-790.
13. X. Yan, X. Wu, Y. Fang, W. Sun, C. Yao, Y. Wang, X. Zhang and Y. Song, *Opt. Mater.*, 2020, **108**, 110171.
14. M. Diao, H. Li, X. Gao, R. Hou, Q. Cheng, Z. Yu, Z. Huang and C. Zhang, *Adv. Funct. Mater.*, 2021, **31**, 2106930.